

Efficient implementation of the concentration-dependent embedded atom method for molecular dynamics and Monte-Carlo simulations

Alexander Stukowski¹, Babak Sadigh², Paul Erhart² and Alfredo Caro²

¹ Institut für Materialwissenschaft, Technische Universität Darmstadt, Darmstadt, Germany

² Lawrence Livermore National Laboratory, Livermore, California 94551, USA

E-mail: stukowski@mm.tu-darmstadt.de

Abstract. The concentration-dependent embedded atom method (CD-EAM) is a powerful model for atomistic simulation of concentrated alloys with arbitrarily complex mixing enthalpy curves. In this paper, we show that in spite of explicit three-body forces, this model can be implemented quite simply with a computational efficiency comparable with the standard EAM for molecular-dynamics simulations. Ready-to-use subroutines for the parallel molecular dynamics code LAMMPS can be provided by the authors upon request. We further propose an improved version of this potential that allows for very efficient calculations of single-particle displacement/transmutation energies, while retaining the complexity implicit in the three-body interactions. This enables large-scale Monte Carlo simulations of alloys with the interatomic interactions described by the CD-EAM model.

Please cite as *Modelling Simul. Mater. Sci. Eng.* 17 (2009), 075005
<http://dx.doi.org/10.1088/0965-0393/17/7/075005>

1. Introduction

Atomistic computer simulations are an important tool to study complex phenomena in physics, chemistry, biology, and materials science. In contrast to *ab-initio* methods, which can be applied to systems containing at most a few hundred atoms, semi-empirical interatomic potentials enable us to simulate systems containing millions of atoms on the time scale of nanoseconds. Large-scale molecular dynamics (MD) and Monte-Carlo (MC) simulations of metals and alloys often make use of the embedded-atom method (EAM) to calculate the interatomic energies and forces. Concentrated alloys which display a non-trivial concentration dependence in the heat of formation (HOF) are, however, beyond the scope of standard EAM models. In the standard EAM scheme, alloying effects are described in terms of the mixed pair interaction that has traditionally been adjusted to the heat of solution of a single impurity (dilute limit). Due to this constraint the standard EAM model cannot be adjusted to describe the inversion in the sign of the HOF of binary alloys such as Fe–Cr and Ni–Pd.

The concentration-dependent model (CD-EAM) developed by Caro *et al.* [1] and first applied to the Fe–Cr system is an attempt to remedy this shortcoming. In this scheme the pair potential for the mixed interaction is assumed to be the product of a function of the interatomic distance and the local concentration $h(x)$. This approach is particularly appealing since it is rooted in the Redlich-Kister expansion of the HOF used to describe alloys beyond the regular solution model. The introduction of the function $h(x)$, which can be obtained with minimal effort, allows the model to reproduce arbitrarily complex HOF curves.

An alternative approach to reproduce the complex shape of the HOF in Fe–Cr was proposed by Olsson *et al.* based on the two-band model (2B-EAM) originally developed by Ackland and Reed [2] to describe materials with both *s*- and *d*-electron states at the Fermi energy. Both the CD-EAM and the 2B-EAM models have successfully been used at various occasions to study precipitation and ordering phenomena in Fe–Cr [3, 4, 5, 6, 7].

In the literature, it has been argued that the CD-EAM and the 2B-EAM models are equivalent [8]. This equivalence, however, does not pertain to the expressions for the atomic forces. While the 2B-EAM model is a superposition of two EAM functions, the versatility of the CD-EAM total energy expression derives from terms that lead to explicit three-body forces. Straightforward evaluation of these forces in MD simulations requires much increased computational effort compared with the standard EAM. In addition, for MC simulations, the calculation of the energy change resulting from displacement or transmutation (change of chemical identity) of a single atom, involves atoms within twice the range of the potential cutoff, making it impractical for large-scale simulations. In this paper we address the computational issues with the CD-EAM model in two ways: first we derive the analytic expression for the CD-EAM forces and show how to efficiently calculate the three-body forces without a need for evaluating three nested sums, and second by proposing a new formulation of the composition dependence

that reduces the range for the energy calculations to the cutoff radius of the potential, while retaining the complexity implicit in its three-body interactions.

This paper is organized as follows: We introduce the CD-EAM model in section 2. The forces for the CD-EAM model are derived in section 3, with further details given in Appendix A. We discuss the computational efficiency of this model when implemented for MD simulations in section 4. On the basis of benchmark simulations we demonstrate that the computational effort for the CD-EAM model is only slightly higher than the standard EAM model. In section 5 we discuss why the original CD-EAM model is inefficient for MC simulations and show how this shortcoming can be circumvented by a modification of the model. The expressions for the interatomic forces for the modified model are obtained in section 6. The implementation of the modified CD-EAM model in MD and MC simulation codes is the subject of sections 4 and 7. We conclude that the new formulation speeds up the MC simulations by an order of magnitude while it is only slightly faster than the standard formulation when applied to MD simulations.

2. The concentration-dependent embedded atom method (CD-EAM)

We begin by reviewing the CD-EAM potential model in its original form [1]. Analogous to the standard EAM model the total energy for a binary alloy involving elements A and B is given by

$$E = \sum_i^N E_i = \sum_i^N \left[F_{\alpha_i}(\varrho_i) + \frac{1}{2} \sum_{j \neq i} V_{\alpha_i \beta_j}(r_{ij}) \right], \quad (1)$$

where α and β denote the atom types and F_{α} is the embedding function for type α . The total electron density ϱ_i at site i is calculated as

$$\varrho_i = \sum_{j \neq i} \rho_{\alpha_j}(r_{ij}). \quad (2)$$

The pair potentials V_{AA} and V_{BB} for the pure elements are functions of the interatomic distance r_{ij} only, whereas the cross potential V_{AB} depends on both the distance r_{ij} and the local concentration x_{ij} according to

$$V_{AB}(r_{ij}) = h(x_{ij})\phi_{AB}(r_{ij}). \quad (3)$$

The function $h(x)$ is fitted to reproduce the concentration dependence of the HOF. If $h(x) = 1$ the conventional EAM format is recovered. In the original CD-EAM model the cross pair potential ϕ_{AB} was simply chosen as

$$\phi_{AB}(r_{ij}) = \frac{1}{2} [V_{AA}(r_{ij}) + V_{BB}(r_{ij})], \quad (4)$$

although in principle this function can be fitted as well. The local concentration of B atoms x_{ij} is estimated from the partial 'B electron densities' at sites i and j ,

$$x_{ij} = \frac{1}{2}(x_i + x_j) = \frac{1}{2} \left(\frac{\varrho_i^B}{\varrho_i} + \frac{\varrho_j^B}{\varrho_j} \right) \quad (5)$$

with

$$\varrho_i^B = \sum_{j \neq i} \rho_{\alpha_j}(r_{ij}) \delta_{\alpha_j B}. \quad (6)$$

The Kronecker symbol $\delta_{\alpha_j B}$ in (6) equals 1 if atom j is of type B and equals 0 otherwise, i.e., the partial density ϱ_i^B includes only contributions from B atoms within the neighborhood of site i . Since the scaling function $h(x_{ij})$ and thus the pair interaction depends on the *local* concentration, the CD-EAM model can handle situations with a spatially varying composition including e.g., interfaces and precipitation processes.

To simplify the following derivations we introduce a shorthand notation for the site energies which can be split into three distinct parts:

$$E_i = F_i + v_i/2 + \bar{v}_i/2. \quad (7)$$

The energy of atom i comprises its embedding energy $F_i = F_{\alpha_i}(\varrho_i)$, its pair interaction sum v_i with atoms of the same species

$$v_i = \sum_{j \neq i} \delta_{\alpha_i \beta_j} V_{\alpha_i \alpha_i}(r_{ij}), \quad (8)$$

and its complementary pair interaction sum \bar{v}_i with atoms of the other species

$$\bar{v}_i = \sum_{j \neq i} \overline{\delta_{\alpha_i \beta_j}} h(x_{ij}) \phi_{AB}(r_{ij}). \quad (9)$$

Here, the Kronecker symbol $\delta_{\alpha_i \beta_j}$ and its counterpart $\overline{\delta_{\alpha_i \beta_j}} = 1 - \delta_{\alpha_i \beta_j}$ have been used to differentiate between the case of two atoms of the same species and the case of two atoms of different species. The per-atom quantity v_i includes all pair-wise interactions of atom i with its neighbors of the same species, whereas \bar{v}_i includes all cross interactions scaled by the concentration dependent factor $h(x_{ij})$.

Closer inspection of the total energy expression [Equations (1)-(6)] reveals that it contains three nested sums over atoms akin to a full-fledged three-body potential. In the present case, the absence of angular dependent terms, however, allows us to decompose the three-body sum into simple pairwise sums. As a result, the energy of the system can be calculated almost as efficiently as in the classical EAM model. Analogous to the latter model only two consecutive loops over all atom pairs are required to calculate all site energies simultaneously.

3. Derivation of forces for the CD-EAM model

For the sake of computational efficiency of MD simulations it is highly advantageous if the interatomic forces can be computed analytically. In this section we give a short description of the computation of the forces for the CD-EAM model. Further details can be found in Appendix A. It is shown that the final expression for the forces can be broken down into pairwise sums in the same way as it is usually done for the standard EAM model. This allows for a very efficient calculation of the CD-EAM forces using three major computational steps:

- Step I. Compute and store the local electron density ϱ_i and partial density ϱ_i^B for each atom i ,

$$\varrho_i = \sum_{l \neq i} \rho_{\alpha_l}(r_{il}) \quad (10)$$

$$\varrho_i^B = \sum_{l \neq i} \rho_{\alpha_l}(r_{il}) \delta_{\alpha_l B}. \quad (11)$$

For performance reasons the derivative $F'_{\alpha_i}(\varrho_i)$ of the embedding energies should also be calculated at this stage and stored for later use in Step III.

- Step II. Compute and store the following per-atom quantity,

$$M_i = \frac{1}{\varrho_i^2} \sum_{j \neq i} h'(x_{ij}) \phi_{AB}(r_{ij}) \overline{\delta_{\alpha_i \beta_j}}. \quad (12)$$

- Step III. Compute the force $\vec{f}_k = -\frac{\partial E}{\partial \vec{r}_k}$ acting on each atom k ,

$$\begin{aligned} \vec{f}_k = - \sum_{i \neq k} \frac{\vec{r}_{ki}}{r_{ki}} & \left[F'_{\alpha_k}(\varrho_k) \rho'_{\alpha_i}(r_{ki}) + F'_{\alpha_i}(\varrho_i) \rho'_{\alpha_k}(r_{ki}) \right. \\ & + \delta_{\alpha_k \beta_i} \cdot V'_{\alpha_k \alpha_k}(r_{ki}) + \overline{\delta_{\alpha_k \beta_i}} \cdot h(x_{ki}) \phi'_{AB}(r_{ki}) \\ & + M_k \cdot \rho'_{\alpha_i}(r_{ki}) [\varrho_k \delta_{\alpha_i B} - \varrho_k^B] / 2 \\ & \left. + M_i \cdot \rho'_{\alpha_k}(r_{ki}) [\varrho_i \delta_{\alpha_k B} - \varrho_i^B] / 2 \right]. \quad (13) \end{aligned}$$

Implementing these three steps in an MD code is straightforward and can be done on top of an existing EAM force routine. In the next section, we show that the computational cost for evaluating the CD-EAM forces in this way is only slightly larger than for conventional EAM models.

4. Molecular dynamics performance

We have implemented two different formulations of the CD-EAM potential model in the popular massively-parallel MD code LAMMPS [9] to compare their computational performance with the standard EAM model. In this section we only discuss the standard CD-EAM model, hereafter referred to as the two-site CD-EAM model. To benchmark its performance, we have carried out MD simulations of a bcc crystal at 300 K using periodic boundary conditions. For the CD-EAM case we considered a random alloy with 50% Cr. For the standard EAM case, the sample contained only Fe. Simulations were run on 1, 8, 27, 64, and 512 processors with 16,000 atoms per processor (weak scaling). The results for the CD-EAM routines and the LAMMPS standard EAM routine are displayed in figure 1. The two-site CD-EAM model is only about 73% slower than the standard EAM model. This is a small price considering the fact that the CD-EAM expression actually contains explicit three-body forces.

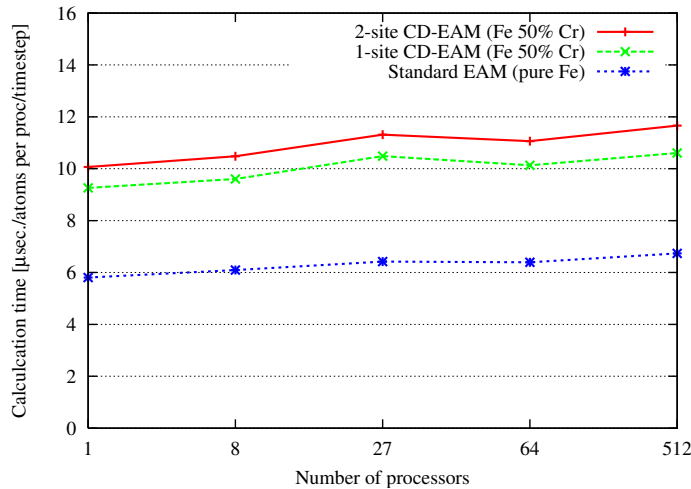


Figure 1. Comparison of the computation times for the CD-EAM models and the standard EAM model in a parallel molecular dynamics simulation. The benchmark simulation consists of a bcc crystal at 300 K with 16,000 atoms per processor.

5. From the two-site concentration model to the one-site concentration model

In the original formulation of the CD-EAM model the $h(x_{ij})$ function depends on the *average* concentration x_{ij} at the two sites i and j [see Equation (5)]. In section 2 it was pointed out that the calculation of the total potential energy is almost as straightforward as for the standard EAM case. But for the following two important reasons it turns out that this simultaneous dependency on two concentrations x_i and x_j is disadvantageous:

- (i) In a MC simulation one frequently needs to calculate the change in total energy, ΔE , resulting from a modification of the system. For most types of MC trial moves (atomic displacement, atom type exchange) the energy change ΔE is local. For performance reasons the calculation of ΔE is usually done by re-evaluating only those site energies that are immediately affected by the move. If one uses the original CD-EAM model the local concentration is computed as the average over the pair $i - j$ which implies that the effective range of the pair interaction is twice as large as the cutoff radius of the potential. While this definition is of little consequence for MD simulations in which the forces are calculated for *all* atoms at once, this definition implies that for the CD-EAM the calculation of local energy changes is much more expensive than for conventional EAM models (for which the effective pair interaction range is identical to the cutoff radius).
- (ii) In section 3 it was shown that the calculation of the atomic forces for the CD-EAM model requires three loops over all atom pairs in the system. This is one step more than for the standard EAM model which requires only two consecutive passes: the first one to calculate the derivatives of the embedding energies and the second one to calculate the forces. For the CD-EAM model one additional computational

step—and in a parallel implementation one additional communication call—are required to calculate the forces.

To summarize these arguments, although the CD-EAM is, in general, employable in large-scale MD studies, there is still room for improvement, and more importantly, its long-range character renders the model prohibitively expensive in the context of MC simulations.

Both of these shortcomings are remedied if one applies the following modification to the CD-EAM model. In Equation (3) we make the replacement

$$h\left(\frac{x_i + x_j}{2}\right) \rightarrow \frac{h(x_i) + h(x_j)}{2}. \quad (14)$$

That is, instead of evaluating the function $h(x)$ at the average concentration of sites i and j , the average value of the $h(x)$ function at the two individual sites is taken to scale the A-B pair interaction. As a result, the individual site energies no longer depend on the local concentration at the neighboring sites. This can be shown by means of the identity

$$\sum_i^N \sum_{j \neq i} \frac{h(x_i) + h(x_j)}{2} \phi_{AB}(r_{ij}) = \sum_i^N h(x_i) \sum_{j \neq i} \phi_{AB}(r_{ij}). \quad (15)$$

The new site energy E_i^* then becomes

$$E_i^* = F_{\alpha_i}(\varrho_i) + v_i/2 + h(x_i)\bar{v}_i^*/2 \quad (16)$$

with

$$v_i = \sum_{j \neq i} \delta_{\alpha_i \beta_j} V_{\alpha_i \alpha_i}(r_{ij}), \quad (17)$$

$$\bar{v}_i^* = \sum_{j \neq i} \overline{\delta_{\alpha_i \beta_j}} \phi_{AB}(r_{ij}). \quad (18)$$

The per-atom quantity v_i includes all pair-wise interactions of atom i with its neighbors of the same species, whereas \bar{v}_i^* includes all cross interactions scaled by the *same* concentration dependent factor $h(x_i)$ after the summation. This property of the site energy expression reduces the computational costs of the new CD-EAM formulation considerably, in particular in MC simulations. We refer to the new model as the *one-site* formulation, since the scaling function $h(x_i)$ is now a function of the local concentration at site i only. A detailed discussion of the performance aspects of this new formulation can be found in sections 6 and 7.

The substitution (14) corresponds to a linearization of the $h(x)$ function. Thus, as long as the concentration does not vary much from site i to site j , or if $h(x)$ is a rather smooth function of the local concentration, the effect of this replacement on the ij -pair energy is very small. It is therefore expected that the one-site CD-EAM model will give almost the same results as the two-site formulation when using the same parametrization.

The original CD-EAM model was developed for the Fe–Cr system. In [1] it was demonstrated that a CD-EAM potential can be fitted such that it exactly reproduces

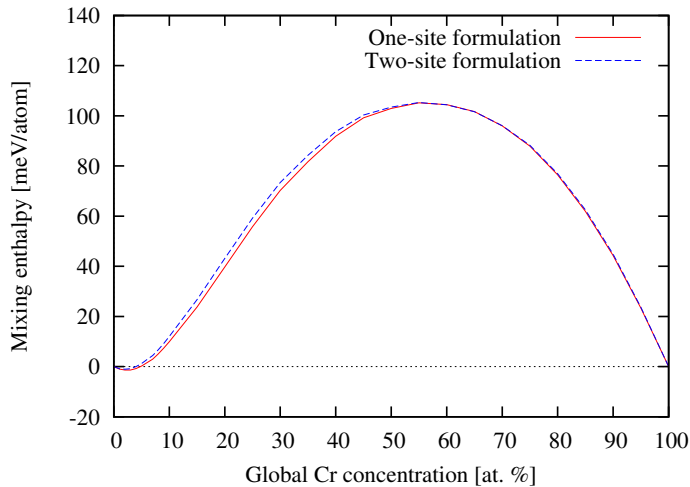


Figure 2. Formation energy for a Fe–Cr random alloy as a function of Cr concentration computed with the one-site and the two-site formulations of the CD-EAM model. The same scaling function $h(x)$ from [1] has been used in both cases. After fitting a new $h(x)$ function (as shown in figure 5) the one-site model yields exactly the same formation energy as the two-site model at all concentrations.

Table 1. Coefficients of the 4th order polynomial $h(x)$ for the Fe–Cr potential in the one-site formulation. Here, x denotes the Cr concentration.

h_0	h_1	h_2	h_3	h_4
1.054732	-1.046606	2.886359	-3.445396	1.450731

the shape of the input HOF curve at all concentrations. Based on the same EAM potentials for pure Fe [10] and Cr [11], and the $h(x)$ polynomial specified in [1] we have re-calculated the mixing enthalpy curve for the random alloy using the new one-site concentration CD-EAM formulation. The result, shown in figure 5, confirms that the proposed reduction to a single site dependency has a minor effect on the resulting mixing enthalpy. As expected, the difference between the two versions of the CD-EAM model is largest at concentrations between 20 and 30 at. % Cr, in the range in which the curvature of $h(x)$ is large (see figure 5). At concentrations above 50% Cr both models yield virtually the same result because the $h(x)$ function is almost constant, and therefore linear, in this composition range.

In order to further improve the one-site formulation, we re-fitted the $h(x)$ function using a least-square algorithm and a 4th order polynomial. The result is shown in figure 5 in comparison to the original polynomial of the two-site Fe–Cr potential [1]. The polynomial coefficients are given in table 1. As expected, inspection of the re-fitted $h(x)$ curve reveals that they differ the most in regions of large curvature. Recalculation of the random alloy formation energy based on the $h(x)$ function gives an exact match with the target curve, meaning that both formalisms are equally suitable to fit a given HOF.

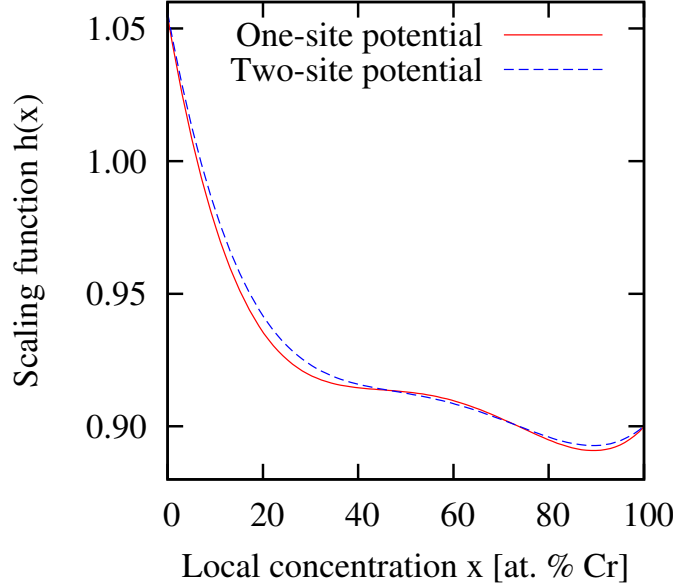


Figure 3. The $h(x)$ scaling polynomial for the original two-site Fe–Cr potential from [1] and the newly fitted polynomial for the one-site formulation. The nonlinear parts of the new curve are more pronounced to compensate for the larger fluctuations of the single site concentrations x_i in the random alloy.

6. The forces for the one-site CD-EAM model

In Appendix B we give the necessary steps for the force derivation for the new one-site formulation of the CD-EAM model. Based on the expression for the interatomic forces, we now demonstrate that the calculation of the interatomic forces requires only two loops over all atom pairs (as opposed to three loops required for the two-site formulation). The necessary computational steps are,

- Step I. Compute and store the local electron density ϱ_i , the partial density ϱ_i^B , and the value \bar{v}_i^* for each atom i :

$$\varrho_i = \sum_{l \neq i} \rho_{\alpha_l}(r_{il}) \quad (19)$$

$$\varrho_i^B = \sum_{l \neq i} \rho_{\alpha_l}(r_{il}) \delta_{\alpha_l B} \quad (20)$$

$$\bar{v}_i^* = \sum_{j \neq i} \overline{\delta_{\alpha_i \beta_j}} \phi_{AB}(r_{ij}). \quad (21)$$

The derivative $F'_{\alpha_i}(\varrho_i)$ of the embedding energy should also be calculated at this point and stored for later use.

- Step II. Compute the force acting on each atom k ,

$$-\vec{f}_k = \sum_{i \neq k} \frac{\vec{r}_{ki}}{r_{ki}} \left[F'_{\alpha_k}(\varrho_k) \rho'_{\alpha_i}(r_{ki}) + F'_{\alpha_i}(\varrho_i) \rho'_{\alpha_k}(r_{ki}) \right]$$

$$\begin{aligned}
& +\delta_{\alpha_k\beta_i} V'_{\alpha_k\alpha_k}(r_{ki}) + \frac{\delta_{\alpha_k\beta_i}}{\delta_{\alpha_k\beta_i}} \frac{h(x_k) + h(x_i)}{2} \phi'_{AB}(r_{ki}) \\
& + \bar{v}_k^* \frac{h'(x_k)}{2\varrho_k^2} \cdot \rho'_{\alpha_i}(r_{ki}) \{ \varrho_k \delta_{\alpha_i B} - \varrho_k^B \} \\
& + \bar{v}_i^* \frac{h'(x_i)}{2\varrho_i^2} \cdot \rho'_{\alpha_k}(r_{ki}) \{ \varrho_i \delta_{\alpha_k B} - \varrho_i^B \} \Big]. \tag{22}
\end{aligned}$$

Since it requires only two consecutive loops over all atom pairs, the new one-site concentration CD-EAM model yields a superior simulation performance, as will be demonstrated in the following.

7. MD/MC performance of the one-site CD-EAM

In section 4, we have already discussed the MD performance of the two-site model. We concluded that in spite of its explicit three-body nature, the two-site CD-EAM model is only a modest 73% slower than the corresponding EAM model, if implemented optimally. In Fig. 1, we also show the performance of the one-site CD-EAM model. The latter is only 60% slower than EAM, mainly because it does not require the additional third loop over all atom pairs to compute the forces as discussed in section 5.

Molecular dynamics simulations are limited when it comes to modeling phenomena such as precipitation, surface and grain boundary segregation, or ordering in alloys. Monte-Carlo (MC) methods, however, are ideally suited for such applications. The most common techniques are based on so-called swap trial moves, in which the chemical identity of a random particle is changed. The resulting change in potential energy, ΔE , is used to decide whether the swap is accepted or rejected.

The main task in a MC simulation is therefore to calculate the change in potential energy induced by swapping the type of a single atom. For short-range potentials this can be done very efficiently, since the type exchange only affects the atoms in the neighborhood of the type swap. In the framework of the standard EAM model the situation is as follows: Changing the species of one atom directly affects (1) its embedding energy, (2) its pair-wise interactions with neighboring atoms, and (3) indirectly changes the electron density at neighboring atoms and therefore their embedding energies. All these quantities need to be recalculated by visiting the atoms affected by the type swap.

In the case of the two-site CD-EAM model the situation turns out to be more laborious. Here, the site energy E_k of an atom k does not only depend on the local concentration x_k , but also on the concentrations x_j of all its neighbors j . This has a dreadful impact on the efficiency of the energy calculation. Changing the chemical identity of some atom i alters the local concentrations x_j of all its direct neighbors j , which in turn affects the mixed interaction of all atoms j with all of their respective neighbor atoms k . All of these have to be re-evaluated to compute the total change in energy induced by the single swap operation. The influence radius that has to be considered is therefore twice as large as the cutoff radius of the underlying EAM potential

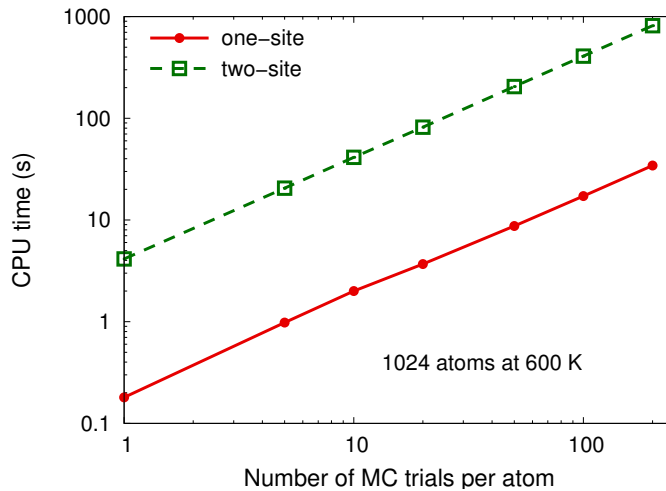


Figure 4. Comparison of the timing in a MC simulation of a Fe-Cr alloy at 50% composition. The simulation cell contained 1024 atoms.

which – for the Fe–Cr potential – increases the computational costs by at least one order of magnitude.

The new one-site formulation proposed in section 5 resolves this issue. Although a single pair interaction between two atoms j and k still depends on the concentration at both sites [see Equation (14)], the site energy can be recast in a form that is independent of the concentrations on the neighboring sites [see Equation (16)]. As a result, the site energy of atom k is no longer affected by changing the type of an atom i that is farther away than one cutoff radius.

The performance gain due to the one-site formulation is illustrated in figure 4 which compares the timing of the one and two-site CD-EAM models in a serial MC simulation for a random Fe-Cr alloy at 50% composition. In this case the one-site CD-EAM model is twelve times faster than the two-site formulation.

We therefore advocate for the new one-site concentration version of the CD-EAM potential which exhibits superior performance in MD and especially MC simulations while preserving all advantages of the original (two-site) CD-EAM model. This model will enable large-scale MD and MC simulations of concentrated alloys and their complex thermodynamic and mechanical properties.

8. Summary and conclusions

We derived the analytic force expression for the concentration-dependent embedded atom method (CD-EAM) potential and showed that the forces for this advanced many-body model can be calculated in a computationally efficient manner, at a cost which is only slightly larger than for standard EAM potentials. This facilitates the application of the CD-EAM model in large-scale molecular dynamics simulations of concentrated alloys.

The CD-EAM model in its original form is not suitable for Monte-Carlo simulations since its effective pair interaction range is twice as large as the cutoff radius of the potential. By introducing a slight modification of the analytic form of the CD-EAM model it is, however, possible to reduce the effective interaction radius to be equal to the cutoff radius. This renders massively-parallel Monte-Carlo simulation based on the new CD-EAM model possible while preserving all of the qualities of the original CD-EAM model.

Energy and force calculation routines for the two-site and the new one-site CD-EAM model have been implemented in the massively-parallel molecular dynamics code LAMMPS [9] and are available upon request from the authors.

Acknowledgments

This work was performed with the financial support of the Deutsche Forschungsgemeinschaft (FOR714) and the German Academic Exchange Service. Lawrence Livermore National Laboratory is operated by Lawrence Livermore National Security, LLC, for the U.S. DOE-NNSA under Contract DE-AC52-07NA27344.

Appendix A. Derivation of the forces for the two-site concentration model

The force \vec{f}_k acting on atom k is given by

$$-\vec{f}_k = \frac{\partial E}{\partial \vec{r}_k} = \sum_i^N \frac{\partial E_i}{\partial \vec{r}_k} \quad (\text{A.1})$$

The terms F_i and v_i in the site energy expression (7) are part of the standard EAM model, so only the third term \bar{v}_i needs special attention when doing the force derivation for the CD-EAM model. We begin by considering the derivative of the product $h(x_{ij})\phi_{AB}(r_{ij})$ from Equation (9) with respect to the position \vec{r}_k of some atom k :

$$\begin{aligned} \frac{\partial}{\partial \vec{r}_k} [h(x_{ij})\phi_{AB}(r_{ij})] = \\ h'(x_{ij})\phi_{AB}(r_{ij})\frac{1}{2} \left[\frac{\partial x_i}{\partial \vec{r}_k} + \frac{\partial x_j}{\partial \vec{r}_k} \right] + h(x_{ij})\phi'_{AB}(r_{ij})\frac{\partial r_{ij}}{\partial \vec{r}_k} \end{aligned} \quad (\text{A.2})$$

The i - j -symmetry of the first term in Equation (A.2) can be exploited in the context of a double sum. One can then do the simplification

$$\sum_{i,j \neq i} \frac{1}{2} \left[\frac{\partial x_i}{\partial \vec{r}_k} + \frac{\partial x_j}{\partial \vec{r}_k} \right] = \sum_{i,j \neq i} \frac{\partial x_i}{\partial \vec{r}_k}. \quad (\text{A.3})$$

Thus we only have to differentiate the concentration at site i :

$$\frac{\partial x_i}{\partial \vec{r}_k} = \frac{\partial}{\partial \vec{r}_k} \frac{\varrho_i^B}{\varrho_i} = \frac{1}{\varrho_i^2} \sum_{l \neq i} [\rho'_{\alpha_l}(r_{il})\delta_{\alpha_l B} \varrho_i - \rho'_{\alpha_l}(r_{il})\varrho_i^B] \frac{\partial r_{il}}{\partial \vec{r}_k} \quad (\text{A.4})$$

with

$$\frac{\partial r_{il}}{\partial \vec{r}_k} = \frac{\vec{r}_{il}}{r_{il}} [\delta_{ki} - \delta_{kl}]. \quad (\text{A.5})$$

At this point, calculating the force $\vec{f}_k = -\frac{\partial E}{\partial \vec{r}_k}$ for a *single* atom k would require the evaluation of three nested sums over the indices i, j , and l (found in equations A.1, 9, A.4). But by incorporating the Kronecker deltas and by decoupling terms with independent indices we now prove that the computational complexity can be reduced to a single sum over index i .

Again we focus on the derivative of the cross potential term only (Equation (A.2)), now in its full form, including both sums over i and j :

$$\begin{aligned} \sum_i \frac{\partial \bar{v}_i}{\partial \vec{r}_k} &= \sum_i \sum_{j \neq i} \overline{\delta_{\alpha_i \beta_j}} \left[h(x_{ij}) \phi'_{AB}(r_{ij}) \frac{\vec{r}_{ij}}{r_{ij}} [\delta_{ki} - \delta_{kj}] \right. \\ &\quad \left. + \sum_{l \neq i} h'(x_{ij}) \phi_{AB}(r_{ij}) \frac{1}{\varrho_i^2} \rho'_{\alpha_l}(r_{il}) \{ \delta_{\alpha_l B} \varrho_l - \varrho_l^B \} \frac{\vec{r}_{il}}{r_{il}} [\delta_{ki} - \delta_{kl}] \right] \end{aligned} \quad (\text{A.6})$$

The four Kronecker deltas in square brackets allow to eliminate one nested sum each, leaving only a double sum after renaming the indices:

$$\begin{aligned} \sum_i \frac{\partial \bar{v}_i}{\partial \vec{r}_k} &= \sum_{i \neq k} \overline{\delta_{\alpha_k \beta_i}} \left[h(x_{ki}) \phi'_{AB}(r_{ki}) \frac{\vec{r}_{ki}}{r_{ki}} - h(x_{ik}) \phi'_{AB}(r_{ki}) \frac{\vec{r}_{ik}}{r_{ik}} \right. \\ &\quad \left. + \sum_{j \neq i} \left\{ h'(x_{ki}) \phi_{AB}(r_{ki}) \frac{1}{\varrho_k^2} \rho'_{\alpha_j}(r_{kj}) \{ \delta_{\alpha_j B} \varrho_k - \varrho_k^B \} \frac{\vec{r}_{kj}}{r_{kj}} \right. \right. \\ &\quad \left. \left. - h'(x_{ij}) \phi_{AB}(r_{ij}) \frac{1}{\varrho_i^2} \rho'_{\alpha_k}(r_{ik}) \{ \delta_{\alpha_k B} \varrho_i - \varrho_i^B \} \frac{\vec{r}_{ik}}{r_{ik}} \right\} \right] \end{aligned} \quad (\text{A.7})$$

The first two terms can be merged into one due to $\vec{r}_{ik} = -\vec{r}_{ki}$. In the inner sum's first term of Equation (A.7) the indices i and j can be swapped without changing the value of the double sum. After this, terms that do no longer depend on index j can be moved out of the inner sum and the remaining part including the j -sum can be given a new name by defining the following per-atom quantity:

$$M_i = \frac{1}{\varrho_i^2} \sum_{j \neq i} h'(x_{ij}) \Phi_{AB}(r_{ij}) \overline{\delta_{\alpha_i \beta_j}}. \quad (\text{A.8})$$

Substituting this back into Equation (A.7) leads to the simplified expression

$$\begin{aligned} \sum_i \frac{\partial \bar{v}_i}{\partial \vec{r}_k} &= \sum_{i \neq k} \frac{\vec{r}_{ki}}{r_{ki}} \left[\overline{\delta_{\alpha_k \beta_i}} \cdot h(x_{ki}) \phi'_{AB}(r_{ki}) \right. \\ &\quad \left. + M_k \cdot \rho'_{\alpha_i}(r_{ki}) \{ \varrho_k \delta_{\alpha_i B} - \varrho_k^B \} \right. \\ &\quad \left. + M_i \cdot \rho'_{\alpha_k}(r_{ki}) \{ \varrho_i \delta_{\alpha_k B} - \varrho_i^B \} \right]. \end{aligned} \quad (\text{A.9})$$

The full expression for the force acting on atom k is given in section 3, Equation (13) along with the necessary steps to evaluate it in an efficient manner.

Appendix B. Derivation of the forces for the one-site concentration model

For the one-site formulation of the CD-EAM model the main difference to the standard EAM model is the term $h(x_i)\bar{v}_i^*$ in Equation (16). Therefore, it is sufficient to focus only on this term when doing the differentiation. We begin by considering the derivative of this product with respect to the position \vec{r}_k of some atom k :

$$\begin{aligned} \frac{\partial}{\partial \vec{r}_k} [h(x_i)\bar{v}_i^*] = \\ h'(x_i) \frac{\partial x_i}{\partial \vec{r}_k} \bar{v}_i^* + h(x_i) \sum_{j \neq i} \overline{\delta_{\alpha_i \beta_j}} \phi'_{AB}(r_{ij}) \frac{\partial r_{ij}}{\partial \vec{r}_k}. \end{aligned} \quad (\text{B.1})$$

The derivative of the concentration x_i is the same as for the two-site CD-EAM formulation, cf. Equation (A.4). Again we focus on the derivative of the cross potential term only as given by Equation (B.1), now in its full form, including the outer sum over i from Equation (A.1):

$$\begin{aligned} \sum_i^N \frac{\partial}{\partial \vec{r}_k} [h(x_i)\bar{v}_i^*] = \sum_i \sum_{j \neq i} \overline{\delta_{\alpha_i \beta_j}} \left[h(x_i) \phi'_{AB}(r_{ij}) \frac{\vec{r}_{ij}}{r_{ij}} [\delta_{ki} - \delta_{kj}] \right. \\ \left. + \sum_{l \neq i} h'(x_i) \phi_{AB}(r_{ij}) \frac{\rho'_{\alpha_l}(r_{il})}{\varrho_i^2} \{ \delta_{\alpha_l B} \varrho_i - \varrho_i^B \} \frac{\vec{r}_{il}}{r_{il}} [\delta_{ki} - \delta_{kl}] \right]. \end{aligned} \quad (\text{B.2})$$

The four Kronecker deltas in square brackets allow to eliminate one nested sum each, leaving only a double sum after renaming the indices:

$$\begin{aligned} \sum_i^N \frac{\partial}{\partial \vec{r}_k} [h(x_i)\bar{v}_i^*] = \sum_{i \neq k} \overline{\delta_{\alpha_k \beta_i}} \left[h(x_k) \phi'_{AB}(r_{ki}) \frac{\vec{r}_{ki}}{r_{ki}} - h(x_i) \phi'_{AB}(r_{ki}) \frac{\vec{r}_{ik}}{r_{ik}} \right. \\ \left. + \sum_{j \neq i} \left\{ h'(x_k) \phi_{AB}(r_{ki}) \frac{1}{\varrho_k^2} \rho'_{\alpha_j}(r_{kj}) \{ \delta_{\alpha_j B} \varrho_k - \varrho_k^B \} \frac{\vec{r}_{kj}}{r_{kj}} \right. \right. \\ \left. \left. - h'(x_i) \phi_{AB}(r_{ij}) \frac{1}{\varrho_i^2} \rho'_{\alpha_k}(r_{ik}) \{ \delta_{\alpha_k B} \varrho_i - \varrho_i^B \} \frac{\vec{r}_{ik}}{r_{ik}} \right\} \right]. \end{aligned} \quad (\text{B.3})$$

The first two terms can be merged into one due to $\vec{r}_{ik} = -\vec{r}_{ki}$. In the inner sum's first term the indices i and j can be swapped without changing the value of the double sum. After this, terms that do no longer depend on index j can be moved out of the inner sum and the remaining parts including the j -sum have the same form as Equation (18) and can therefore be replaced by \bar{v}_k^* and \bar{v}_i^* respectively. After this substitution Equation (B.3) gets simplified to

$$\begin{aligned} \sum_i^N \frac{\partial}{\partial \vec{r}_k} [h(x_i)\bar{v}_i^*] = \sum_{i \neq k} \frac{\vec{r}_{ki}}{r_{ki}} \left[\overline{\delta_{\alpha_k \beta_i}} [h(x_k) + h(x_i)] \phi'_{AB}(r_{ki}) \right. \\ \left. + \bar{v}_k^* \frac{h'(x_k)}{\varrho_k^2} \cdot \rho'_{\alpha_i}(r_{ki}) \{ \varrho_k \delta_{\alpha_i B} - \varrho_k^B \} \right. \\ \left. + \bar{v}_i^* \frac{h'(x_i)}{\varrho_i^2} \cdot \rho'_{\alpha_k}(r_{ki}) \{ \varrho_i \delta_{\alpha_k B} - \varrho_i^B \} \right]. \end{aligned} \quad (\text{B.4})$$

The full expression for the force acting on atom k is provided in section 6 along with the necessary steps to evaluate it in an efficient manner.

References

- [1] A. Caro, D. A. Crowson, and M. Caro. Classical many-body potential for concentrated alloys and the inversion of order in iron-chromium alloys. *Phys. Rev. Lett.*, 95(7):075702, 2005.
- [2] G. J. Ackland and S. K. Reed. Two-band second moment model and an interatomic potential for caesium. *Phys. Rev. B*, 67(17):174108, 2003.
- [3] P. Olsson, J. Wallenius, C. Domain, K. Nordlund, and L. Malerba. Two-band modeling of alpha-prime phase formation in Fe-Cr. *Phys. Rev. B*, 72(21):214119, 2005.
- [4] A. Caro, M. Caro, E. M. Lopasso, and D. A. Crowson. Implications of ab initio energetics on the thermodynamics of Fe-Cr alloys. *Appl. Phys. Lett.*, 89(12):121902, 2006.
- [5] M. Yu. Lavrentiev, R. Drautz, D. Nguyen-Manh, T. P. C. Klaver, and S. L. Dudarev. Monte carlo study of thermodynamic properties and clustering in the bcc Fe-Cr system. *Phys. Rev. B*, 75(1):014208, 2007.
- [6] P. Erhart, A. Caro, M. Caro, and B. Sadigh. Short-range order and precipitation in Fe-rich Fe-Cr alloys: Atomistic off-lattice Monte=Carlo simulations. *Phys. Rev. B*, 77(13):134206, 2008.
- [7] G. Bonny, P. Erhart, A. Caro, R. C. Pasianot, L. Malerba, and M. Caro. The influence of short range order on the thermodynamics of Fe-Cr alloys. *Modelling Simul. Mater. Sci. Eng.*, 17:025006, 2009.
- [8] G. Bonny, R. C. Pasianot, and L. Malerba. Interatomic potentials for alloys: Fitting concentration dependent properties. *Phil. Mag.*, 89(8):711, March 2009.
- [9] S. Plimpton. Fast parallel algorithms for short-range molecular dynamics. *J. Comp. Phys.*, 117(1):1, 1995.
- [10] M. I. Mendeleev, S. Han, D. J. Srolovitz, G. J. Ackland, D. Y. Sun, and M. Asta. Development of new interatomic potentials appropriate for crystalline and liquid iron. *Phil. Mag.*, 83(35):3977, 2003.
- [11] J. Wallenius, P. Olsson, C. Lagerstedt, N. Sandberg, R. Chakarova, and V. Pontikis. Modeling of chromium precipitation in Fe-Cr alloys. *Phys. Rev. B*, 69(9):094103, 2004.